論文の内容の要旨

Construction and Control of Hierarchical Systems at the Interfaces on Functionalized Carbon Clusters

（化学修飾炭素クラスター界面における階層化システムの構築と制御）

ゴルゴル　リカルド　ミゾグチ

Introduction

Carbon clusters have been widely used as scaffolds in the construction of hierarchical assemblies of organic and inorganic materials because of their unique shape, stability, and electron conductivity. In this study, I investigated two nanocarbon assemblies of mesoscopic scaffold: 30 nm bilayer vesicles made of fullerene amphiphiles ((R-^{p}C$_6$H$_4$)$_5$C$_{60}^{-}$K^{+}, Fig. 1a) and 100 nm aggregates of carbon nanohorns (Fig. 1b). The functional group introduced to the curved π-surface of fullerene or nanohorn is exposed on the surface of these assemblies, which allows the design of the interface on these clusters and thus control of their properties. In the fullerene vesicles, the [60]fullerene moiety is located in the membrane interior and the R groups are exposed to the aqueous environment, creating three well-defined regions in the bilayer: fullerene-rich core, (perfluoro)alkyl-rich interior and surface. Mutually orthogonal forces, π–π and hydrophobic/fluorous interactions, grant high stability to the fullerene membrane in comparison to others, such as lipid membranes. The carbon nanohorn aggregate has a peripheral morphology displaying carbon nanohorns functionalized with single organic molecules that can be individually visualized by electron microscope.

In this thesis, I developed the chemistry at the interfaces on carbons clusters based on precise molecular design and synthesis. Fullerene vesicles and carbon nanohorn aggregates were applied as scaffolds for selective binding of small molecules, tunable nanoreactors, plasmonic vesicles, and observation of single organic molecule dynamics.

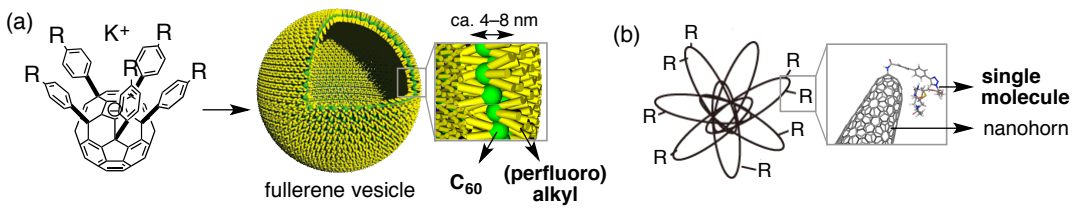

Figure 1. Assemblies of carbon nanoclusters: (a) Fullerene vesicle and (b) carbon nanohorn aggregate.

Binding of aromatic molecules in the fullerene-rich interior of fullerene vesicles

The binding of small molecules to vesicles made of fullerene amphiphiles **1**–**5**, hereafter called **V1**–**V5**, is expected to occur in a way different to vesicles made of lipid molecules, because of the different architecture of the bilayer membranes (Fig. 2). Here, I investigated the binding of aromatic molecules to fullerene bilayer membranes. The part of the membrane that traps organic molecules was determined by using an aromatic fluorescent dye, prodan. The strong quenching of the fluorescence indicates that the vesicle binds aromatic molecules primary in the interior of the fullerene bilayer. The binding profile of the fullerene membrane for hydrocarbons largely depends on the structure of the R group. **V1** and **V2**, which represent an all-aromatic molecular structure lacking the aliphatic substituents, bind naphthalene better than *trans*-decalin. This preference does not reflect the logP_{ow} values and suggests that the naphthalene binding occurs because of an aromatic–fullerene interaction. On the other hand, **V3** and **V4** vesicles bind *trans*-decalin better than naphthalene, suggesting that the primary binding site is the alkyl chains. **V5** has a similar loading profile to **V1** and **V2**, which we ascribe to the flexibility of this vesicle. In addition, the binding of larger aromatic molecules with three-dimensional structures (phenanthrene, biphenyl, *p*-terphenyl) revealed that the vesicles take up a planar molecule very well but not bulky aromatic molecules.

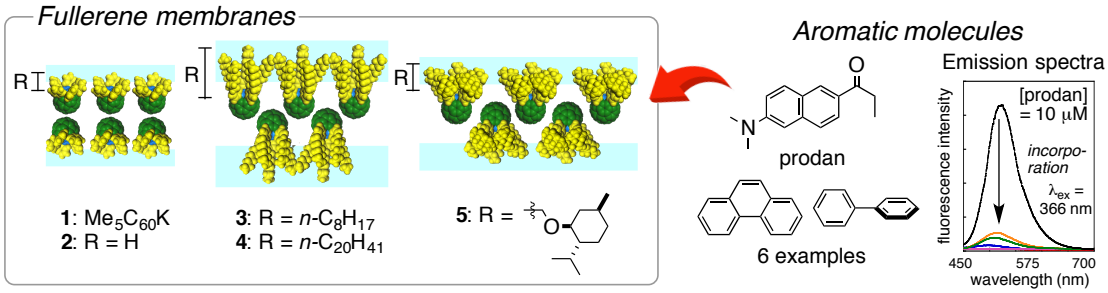

Figure 2. Binding of aromatic molecules to fullerene bilayers made of amphiphiles **1**–**5**.

Control of polymer growth in nm-thick fullerene bilayers

Many reactions in our body occur inside a cell membrane; however, scientists have struggled to use lipid membranes as nanoreactors in flasks because of their structural instability. The high stability of the fullerene vesicle, granted by the orthogonal forces, allowed the control of polymer growth in the different regions of the bilayer (Fig. 3).

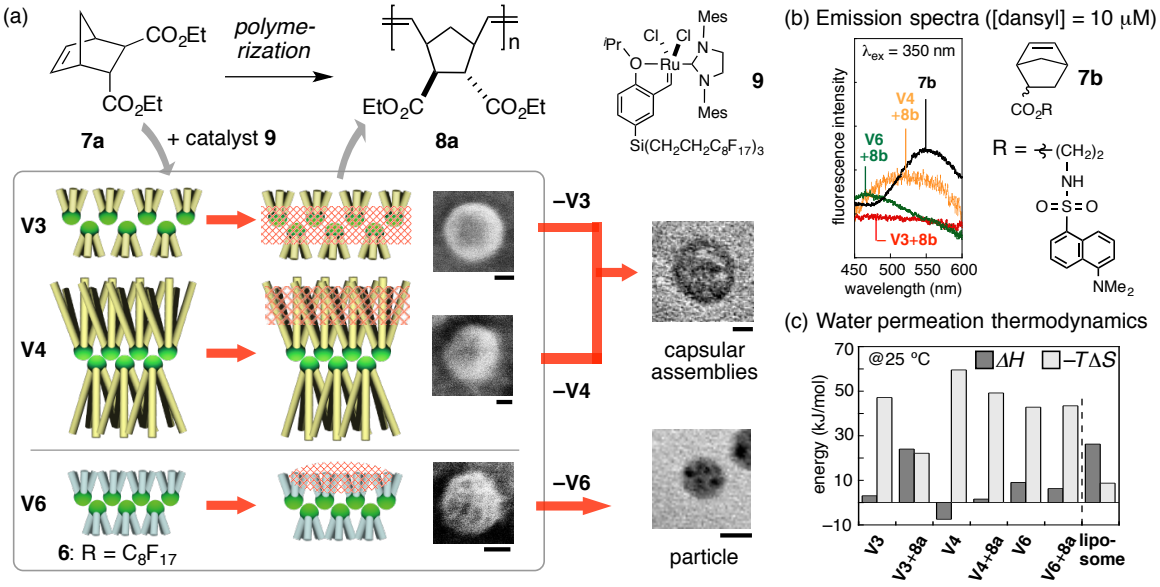

Figure 3. Control of polymer growth in the different regions of the fullerene bilayer. SEM image of the vesicle after ROMP of **7a** and STEM image of polymer **8a** after removal of the vesicle template are shown. Scale bars are 10 nm. The location of the polymer chains in the bilayer was investigated by (b) fluorescence spectra and (c) water permeation profile of fullerene bilayers.

A norbornene dicarboxylate ester (**7a**) was polymerized by a fluorous-tagged Hoveyda-Grubbs' catalyst (**9**, 2 mol%) on fullerene vesicles (1 norbornene per R group) producing polyester **8a** (> 97% conversion) in ring-opening metathesis polymerization (ROMP). The molecular weight of the polymers (ca. 2 x 10^5 g mol^{-1}, $Đ$ = ca. 2) was similar in all cases, indicating that the vesicle did not change the nature of the reaction. The structural stability of the bilayers after the reaction was confirmed by dynamic light scattering (DLS). The vesicle size increased 15 to 31% without significant change to the size distribution. The location of the polymer in the different bilayers was investigated by a fluorescence probe, water permeation and electron microscope studies of the vesicle/polymer composites.

Fluorescence quenching by the fullerene core of the membrane provided information on the location of the polymer chains. After copolymerization of dansyl ester **7b** to **7a** (5:95), the intensity of the dansyl group fluorescence in the vesicle/polymer composite decreased in the order of (**V4**>**V6**>**V3**) (Fig. 3b). Blue-shift of the fluorescence maximum of dansyl group, a measure of the hydrophobicity of the environment, was also stronger at **V4** than at **V6**. Therefore, ROMP in **V3** occurred near the fullerene core, while ROMP in **V4** occurred in the vicinity of the C20 side chains, and in **V6** in the fluorous environment.

Water permeation through a fullerene bilayer is a unique entropy-controlled process. However, after ROMP on **V3,** the water permeation became controlled more by the enthalpy term than by the entropy term, confirming that the polymerization occurred near the fullerene core for this membrane (Fig. 3c). On **V4** and **V6**, the entropy term continued to dominate, as polymerization took place in the side-chain region.

The location of the polymer chains in the membrane affected the final morphology of the polymeric object, extracted as supramolecular capsule or particle. The polymer formed in **V3** was isolated as a 35 nm hollow capsule, while the one formed on **V4** only partially retained the spherical shape, because of the structurally mobility of the C20 side chain region of the bilayer. Polymerization on **V6** produced phase-segregated nodules on the fluorinated surface of the vesicle, which were isolated as 5.5 nm particles.

Cooperative self-assembly of gold nanoparticles on the hydrophobic surface of fullerene vesicles in water

Functionalization of vesicles with inorganic particles is usually achieved by electrostatic interaction between vesicle surface and particles. However, strong repulsion between neighboring particles results in low surface coverage, limiting the applications of such structures. The hydrophobic surface of fullerene vesicles, created by the display of (perfluoro)alkyl chains on the surface, allowed the construction of sub-100 nm plasmonic vesicles densely covered with neutral gold nanoparticles by adsorption on the oil/water interface (Fig. 4).

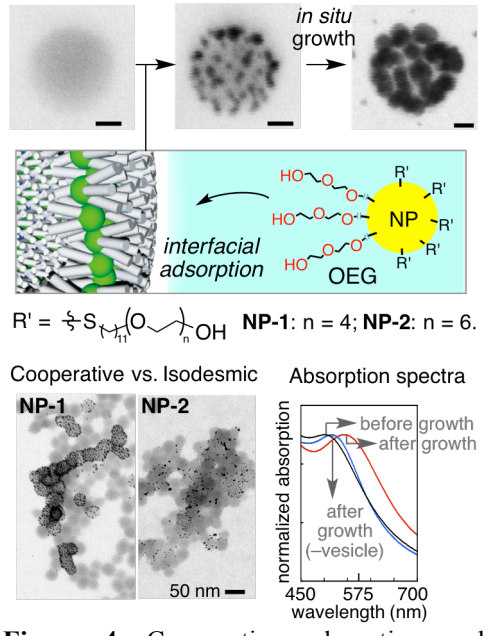

Figure 4. Cooperative adsorption and growth of OEG-coated gold nanoparticles on fullerene vesicles. Scale bars are 10 nm.

3.5 nm water-soluble OEG-coated gold nanoparticles (**NP-1**) cooperatively assembled on the surface of **V6** forming plasmonic vesicles of 50 nm, as shown by electron microscope images. The supramolecular assembly withstands purification by size exclusion chromatography and enhances the vesicle stability in biological conditions (e.g. PBS). The hierarchical structure is also maintained in the solid state after removal of water. The cooperative mechanism was found to be important for the hybrid formation, since the use of **NP-2**, which has longer OEG ligands and thus higher surface activity, caused fusion of the vesicles in an isodesmic adsorption. The high stability was attributed to interparticle interaction mediated by the OEG chains on the nanoparticles, as suggested by NMR experiments.

The nanoparticles were grown in-situ on the vesicle surface into particles of up to 7.2 nm in diameter by addition of a growth solution and a reducing agent to the hybrids. The larger particles resonate on the vesicle surface as the peak of the plasmon absorption shifted from 517 nm (free particles) to 544 nm, suggesting possible application of the hybrids as a new material for imaging.

Observation of dynamic conformational changes of single organic molecules on a carbon nanohorn by low-acceleration voltage TEM

The unique morphology of carbon nanohorn aggregates allows the observation of isolated caps and their functional groups by transmission electron microscope (TEM) in near-atomic resolution. Here, the I envisioned that tuning of TEM conditions and proper molecular design of the functional groups would further allow the experimental observation of the dynamics of single organic molecules, a challenging topic reported only for a few molecules observed by STM.

The dynamics of the molecules were quantified by calculation of the cross correlation between consecutive frames of the TEM movie. This parameter was used for comparison of the dynamics of single molecules in different movies.

In a TEM measurement, the molecule is irradiated by electrons of energy proportional to the acceleration voltage. The conformational changes of **10**, a model molecule, were more significant under an acceleration voltage of 60 kV than of 80 or 120 kV. Therefore, low-energy electrons induce molecular motion more than high-energy electrons. Since low-energy electrons have higher inelastic cross section, the dynamics observed by TEM should be a result of inelastic scattering of the electrons. The generality of this finding was further investigated by other two biotinylated molecules, **11** and **12**, and the dynamics of these molecules were also faster at a lower acceleration voltage.

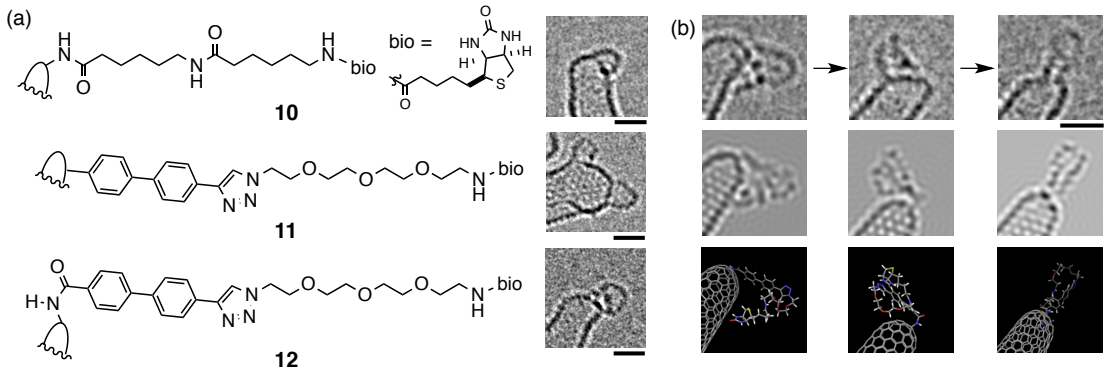

Figure 5. Observation of the dynamics of single molecules by TEM. (a) (left) Molecular structure and (right) TEM images of **10**–**12**. (b) Plausible conformations of TEM images of the molecular motion of **12**. The TEM image is shown in the top, a molecular model of a plausible conformation is shown in the bottom, and its TEM simulation is shown in the middle. Scale bars are 1 nm.

The biphenyl and tetraethylene oxide moieties in **11** and **12**, introduced as rigid and flexible spacers, produced more complex dynamics than **10** (Fig. 5a). At 80 kV, **12** has the fastest conformational changes between the three molecules and **10** has the slowest. Further analysis of the dynamics of **12** (Fig. 5b) and comparison with molecular dynamics simulation suggested that the faster dynamics of this molecular design is a result of the high flexibility of the ethylene glycol spacer, rotation and isomerization of the amide bond, and local conformational minima originated from steric hindrance between biphenyl and the nanohorn surface.

Conclusion

The high stability, facile chemical modification and well-defined scaffold of carbon clusters assemblies allowed the construction of hierarchical systems for diverse applications. The fullerene bilayer vesicle, which is stabilized by orthogonal forces (π-π and hydrophobic/fluorous interactions), was used as a binding site for aromatic molecules, a nanoreactor for the synthesis of polymeric objects, and a scaffold for plasmonic vesicles. The morphology of carbon nanohorn aggregates allowed the experimental observation of the dynamics of single organic molecules in electron microscope, which was controlled by the acceleration voltage and molecular design. The methods developed in this thesis pave the way for a new chemistry made possible by the unique properties of carbon clusters.